Materials Chemistry and Physics xxx (2015) 1–9

Contents lists available at ScienceDirect

Materials Chemistry and Physics

journal homepage: www.elsevier.com/locate/matchemphys

Enhanced compatibility and morphology evolution of the hybrids involving phenolic resin and silicone intermediate

Shan Li [a, b], Fenghua Chen [a], Yue Han [a, b], Heng Zhou [a], Hao Li [a, **], Tong Zhao [a, *]

[a] Laboratory of Advanced Polymer Materials, Institute of Chemistry, Chinese Academy of Sciences, Beijing 100190, PR China
[b] University of Chinese Academy of Sciences, Beijing 100049, PR China

HIGHLIGHTS

- Hybrid resin containing phenolic resin and silicone intermediate was prepared.
- The morphology evolution mechanism of the hybrid during curing was discussed.
- Thermal stability of the cured hybrids was improved.

ARTICLE INFO

Article history:
Received 20 April 2015
Received in revised form
13 July 2015
Accepted 18 July 2015
Available online xxx

Keywords:
Polymers
Heat treatment
Electron microscopy (STEM, TEM and SEM)
Thermal properties

ABSTRACT

In this paper, hybrids containing novolac phenolic resin (NR) and silicone intermediate (SI) were investigated. Compatibility between the two components was enhanced by modifying NR with a coupling agent, γ-(2,3-epoxypropoxy) propyltrimethoxysilane (KH560). SI with silanol groups was synthesized by the hydrolysis of phenyltrimethoxysilane and dimethyldimethoxysilane. Different amount of SI was blended with modified NR, and the corresponding yellow transparent samples were obtained and used for the subsequent curing and microscopic observation. SI-rich nanoparticles were found to be evenly dispersed in the initial sample and further coarsened to nano- and micro-particles. The size and amount of the particles increased with the SI loading. The morphology evolution mechanism was discussed based on microscopic observation and chemical reaction processes. Thermal stability of the cured hybrids was characterized by thermalgravimetric analysis. Temperatures at 5% and 10% mass loss and residual weight at 900 °C were found to increase with the SI loading. Furthermore, carbon retention after high temperature oxidation was also increased.

1. Introduction

Phenolic resin (PR) shows excellent mechanical properties and heat resistance; therefore, it has been widely used as molding compounds, laminate, coating, thermal insulation materials and adhesive [1–3]. However, traditional PR usually possesses poor oxidation resistance and exhibits high volume shrinkage during curing and carbonization, limiting the application of phenolic resin in military and aerospace industries [4,5]. In order to improve its thermal stability, especially high-temperature ablation performance and carbon retention, compounds containing inorganic elements, such as boron [6,7], phosphorous [8] and silicon [9–11] have been introduced into PR.

Polysiloxane is a kind of inorganic polymer with flexible molecular chains, and possesses unique properties, such as good thermal and oxidative stability, flame retardancy, low volume shrinkage [12,13]. Polymer composites modified via polysiloxane possess improved thermal properties [11,13], water resistance [14] and toughness [15]. However, polysiloxane usually shows poor compatibility with organic polymers, and many efforts have been made to solve this problem [16–22], including coupling agent introduction [9,23], chemical group grafting [20,24–26], copolymerization [16,27] and in-situ polymerization [9,18,28]. L. Mascia et al. used the coupling agent, γ-(2,3-epoxypropoxy) propyltrimethoxysilane and partly substituted tetraethoxy-silicone (TEOS) with dimethylethoxysilane to control the morphology of the polyimide/silica hybrid [18]. Co-continuous phase and dispersed particle structures were obtained. The former structure

* Corresponding author.
** Corresponding author.
E-mail addresses: lihao306@iccas.ac.cn (H. Li), tzhao@iccas.ac.cn (T. Zhao).

http://dx.doi.org/10.1016/j.matchemphys.2015.07.054
0254-0584/

was much more effective in reducing the coefficient of thermal expansion while the latter gives higher mechanical strength and ductility. Yong Ni et al. introduced polysilsesquioxane (POSS) grafted amino groups into epoxy resin, and the functional groups reacted with the epoxide group and effectively enhanced the compatibility [25]. Nobuyuki Furukawa copolymerized polysiloxane and polyimide to obtain a block-copolymer, and no macroscopic phase separation was observed [14]. Also, in-situ polymerization method was used to prepare the polymer/silica hybrid resin with fine dispersion and strong interfacial interaction [9]. The morphology evolution of hybrids containing phenolic and polysiloxane has rarely been reported. Yudong Zhang studied the multistep aggregating phase separation process of the phenolic resin/trisilanolphenyl polyhedral oligomeric silsesquioxane (POSS), and proved that the dispersed POSS-rich particles in micron-size were formed by the aggregation of smaller particles together with phenolic resin [10].

The hybridization of phenolic resin and polysiloxane is an effective method to improve the anti-ablative properties of the phenolic resin but the morphology evolution during the curing process remains unknown. In this study, novolac phenolic resin was first modified with a coupling agent γ-(2,3-epoxypropoxy) propyltrimethoxysilane, and subsequently blended with silicone intermediate (SI) synthesized from the prehydrolysis-condensation of phenyltrimethoxysilane and dimethyldimethoxysilane monomer. Fine dispersion of SI-rich nanoparticles was observed in the initially mixed sample and morphology evolution during the curing process was investigated and discussed. Thermal property and oxidation resistance of the cured hybrids were enhanced.

2. Experimental

2.1. Materials

Novolac phenolic resin (PF-8013) was supplied by Shandong Jinan Shengquan Co. Ltd, China. Coupling agent, γ-(2,3-epoxypropoxy) propyltrimethoxysilane (KH560) was purchased from Alfa Aesar Co. Ltd. The silicon intermediate (SI) was synthesized by the hydrolysis-condensation of phenyltrimethoxysilane (PTMS) and dimethyldimethoxysilane (DMDMS), which were obtained from Hubei New Blue Co. Ltd, China. Hexamethylene tetramine (HMTA), the curing agent for the novolac resin and hybrids, was obtained from Sinopharm Chemical Reagent Co. Ltd. All of the chemicals were chemical reagent and used as received.

2.2. Measurements

^{29}Si-NMR spectra was recorded on a Bruker Avance 400 MHz NMR spectrophotometer. Molecular weight and distribution of the silicone intermediate were measured on Waters 1515 Gel Permeation Chromatography (GPC) with tetrahydrofuran as the mobile phase. Fourier Transform Infrared Spectroscopy (FTIR) measurements were performed on a Tensor-27 spectrometer at room temperature. Samples were grinded, mixed with KBr and pressed into the small flakes for testing. Viscosity-time relationship study was performed using a cone-and-plate configuration (Φ20 mm, 1° cone geometry) on an AR-2000 Rheometer at a frequency of 1 Hz. The gap distance between the cone and the plate was fixed at 2.5 mm. Gel time test was conducted on the gel plate. 1 g of sample was stirred on the hot plate until it gelled and this time period was defined as the gelled time. Thermolgravimetric analysis was carried out from ambient temperature to 900 °C on a Netzsch STA409PC at a heating rate of 10 °C min^{-1} in nitrogen atmosphere. Oxidation resistance test was conducted in a muffle furnace at high temperature under air atmosphere. Elemental analysis was performed using a Flash EA 1112 analyzer.

Olympus BX51 phase contrast optical microscopy (PCOM) was used to study the phase structure at preliminary stage. The cured samples were quenched and cracked in liquid nitrogen. Fracture surface of the cured hybrids were sputtered with gold, and observed on a Hitachi S-4800 scanning electron microscope (SEM) at an accelerating voltage of 10 kV. The ultrathin trimmed samples were achieved on an ultramicrotome machine, stained by phosphotungstic acid, and observed on a JEM-2011 transmission electron microscope at an accelerating voltage of 200 kV.

2.3. Synthesis of the modified-novolac resin (m-NR) and silicone intermediate (SI)

Neat novolac-type phenolic resin was dissolved into tetrahydrofuran (THF) to get a solution with 50 wt% resin content. In order to enhance the compatibility between NR and SI, KH560 was used as the coupling agent to modify the phenolic resin. The KH560 loading level was set as 10 per hundred ratio of the novolac resin by weight. Triphenylphosphine was used as the catalyst to promote the coupling reaction. After stirring at 78 °C for about 24 h, m-NR was obtained. The above synthesis involved a ring opening reaction between epoxy groups in KH560 and hydroxyl groups in the phenolic resin, as shown in Scheme 1a. This m-NR/THF solution was designated as solution A.

SI solution was prepared by dissolving PTMS and DMDMS with a molar ratio of 2:1 into THF. Phenyl group in PTMS has potential to increase the compatibility of SI with NR by forming aromatic π-π interactions [4]. Distilled water and hydrochloric acid were used to initiate the hydrolysis of the alkoxy group. The molar ratio of water and alkoxy groups was set as 1:2. SI was obtained by the prepolymerization of PTMS and DMDMS at 30 °C for 20 min. The hydrolysis-condensation reaction was shown in Scheme 1b. The obtained SI solution was designated as solution B.

2.4. Preparation of hybrid resins

Solutions A and B were mixed in different ratio to obtain m-NR/SI prepolymer blends. The curing agent, HMTA, was then added into the mixture with a loading level of 10 per hundred ratio of the m-NR by weight. After refluxing for 4 h, the solvent was removed in vacuum at room temperature, and transparent hybrid resins were obtained. Here, the weight ratio between m-NR and SI was set as 95:5, 85:15, 75:25 and 65:35, and the corresponding blends were designated as 95-5m-NR/SI, 85-15m-NR/SI, 75-25m-NR/SI and 65-35m-NR/SI, respectively.

3. Results and discussion

3.1. Characterization of m-NR and SI

FTIR was used to characterize m-NR, and the spectra were shown in Fig. 1. The characteristic peak at 906 cm^{-1} (corresponding to epoxy group) disappeared after the reaction, suggesting the occurrence of the ring−opening reaction of KH560. The appearing of new signal at 1140 cm^{-1} (corresponding to C−O-phenyl) confirmed the successful reaction between NR and KH560, as shown in Scheme 1a.

Fig. 2 showed the ^{29}Si-NMR spectrum of the SI. The peaks at about −19, −71 and −80 ppm could be attributed to $(CH_3)_2SiO$, HO(ph)SiO and (ph)$SiO_{1.5}$ groups, respectively. The peak at −63 ppm was assigned to the dimmer of phenyltrimethoxysilane [30]. GPC measurements (shown in Fig. 2b) indicated that the number-average molecular weight of SI is 659 corresponding to about 4−5 repeating unit and the molecular weight distribution

Please cite this article in press as: S. Li, et al., Enhanced compatibility and morphology evolution of the hybrids involving phenolic resin and silicone intermediate, Materials Chemistry and Physics (2015), http://dx.doi.org/10.1016/j.matchemphys.2015.07.054

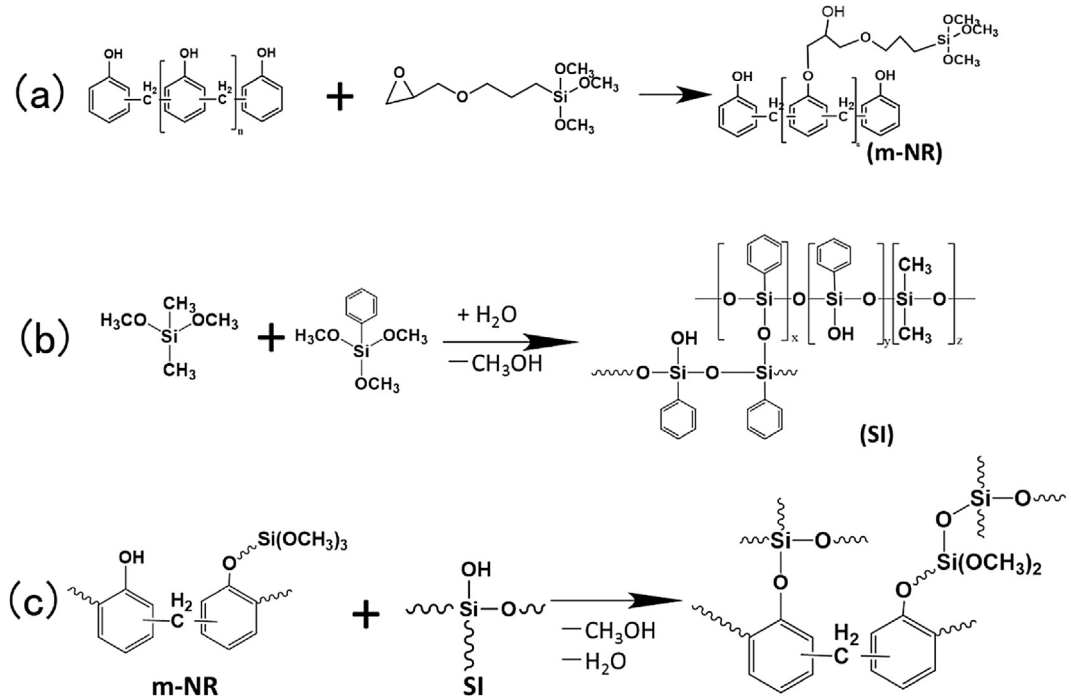

Scheme 1. (a) synthesis of the modified novolac resin; (b) synthesis of the silicone intermediate; (c) the reaction between m-NR and SI.

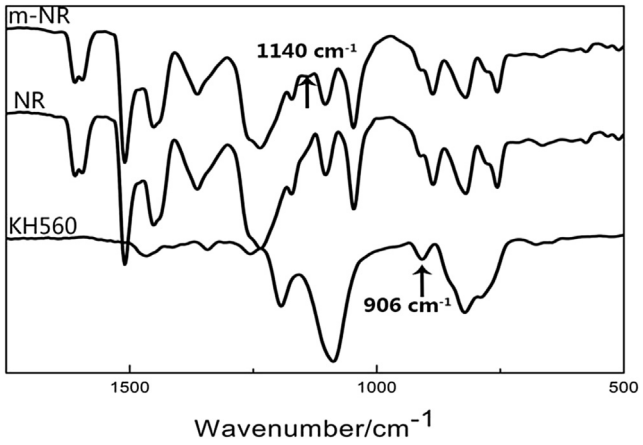

Fig. 1. FTIR spectra of modified novolac resin.

(PDI = 1.10) is narrow. According to the comparison between the GPC curves of monomers (PTMS, DMDMS) and the SI product, the monomers were completely reacted. The alkoxy groups in PTMS and DMDMS were hydrolyzed and silanol groups were formed. Part of the silanol groups self-condensed, as generated Si—O—Si bonds, while other silanol groups remained in the structure, and this process was shown in Scheme 1b. The remaining silanol groups may form hydrogen bond with the phenol group in novolac resin [10,31]. The hydrogen bond and the low molecular weight of SI were beneficial for the SI dispersion in phenolic matrix.

Hybrid resins with different SI loadings were characterized by FTIR, and the spectra were illustrated in Fig. 3. The intensity of the signal at 1135 cm^{-1} (corresponding to the Si—O—Si unit) enhanced with the increase of SI loadings. The intensity of signals at 1595 cm^{-1}, 1435 cm^{-1} could be attributed to the vibration of Si-ph, and 1260 cm^{-1}, 778 cm^{-1} was ascribed to that of Si—CH_3; these signals intensity also slightly increased with the increase of SI contents. Si—OH was hard to be distinguished from OH group in NR.

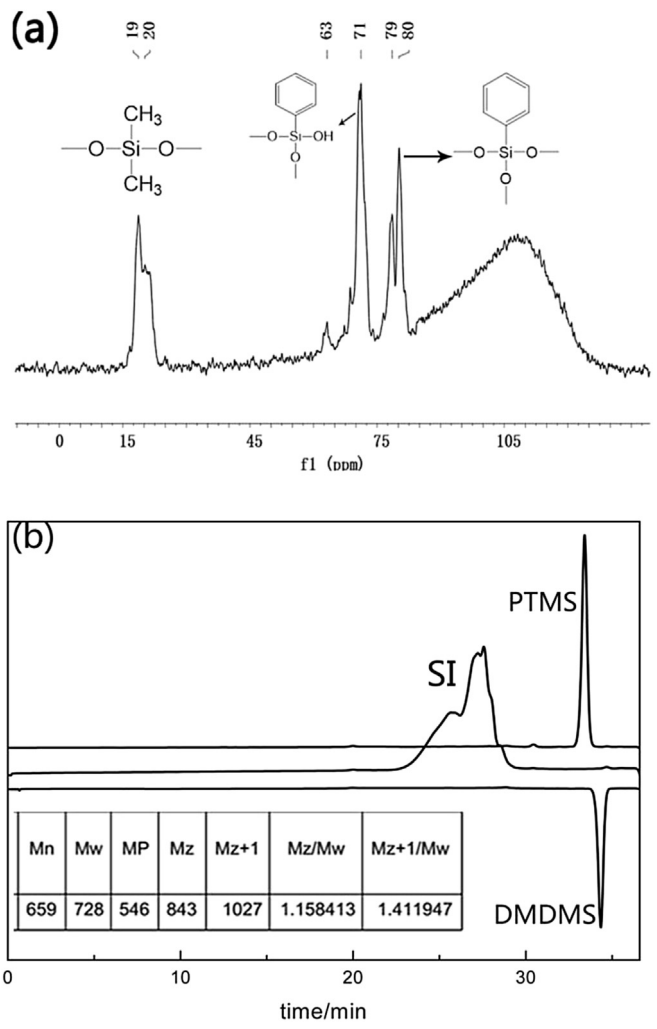

Fig. 2. Chemical structure characterization of SI: (a) ^{29}Si-NMR; (b) GPC spectra.

Please cite this article in press as: S. Li, et al., Enhanced compatibility and morphology evolution of the hybrids involving phenolic resin and silicone intermediate, Materials Chemistry and Physics (2015), http://dx.doi.org/10.1016/j.matchemphys.2015.07.054

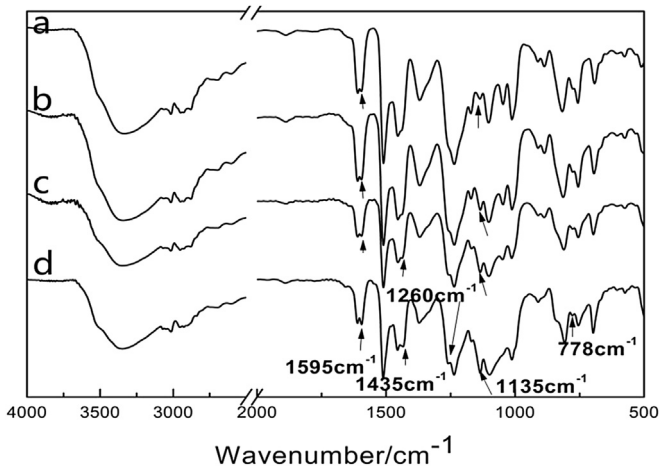

Fig. 3. FTIR spectra of hybrid resins: (a) 95-5m-NR/SI; (b) 85-15m-NR/SI; (c) 75-25m-NR/SI; (d) 65-35m-NR/SI.

3.2. Curing behavior of the hybrids

The coupling of the m-NR and SI influenced the individual reactions and also modulate the dynamic behavior in the curing process. Samples m-NR + HMTA, SI + HMTA and 75-25m-NR/SI were taken as the examples to demonstrate the differences in the curing behavior, and isothermal rheological measurement were performed at 110 °C and illustrated in Fig. 4. The gel point can be defined as the crossover time of the storage modulus (G′) and loss modulus (G″) [32]. According to the rheological curves, the gel time for m-NR + HMTA, SI + HMTA and 75-25m-NR/SI hybrid were 6, 115 and 9 min, respectively. Compared with m-NR, the relatively longer gel time of the hybrid sample was attributed to the dilution effect of SI on the m-NR curing reaction. Generally, the functional conversion rate of novolac resin at the gel point cannot be higher than 40% [33], which means only loose network was formed at this stage. In the present system, self-polymerization of SI and copolymerization between SI and m-NR were much slower than the self-polymerization of the m-NR. It could be implied that during the gel process of the hybrid at 110 °C, the dilution effect of SI played a more significant role, compared with the reaction enhancement of the functional groups. SI still possessed good fluidity at the gel point and could continue to aggregate in the following processes.

Gel times for all hybrids at different temperatures were obtained by gel plate test and the result was shown in Table 1. Gel time was delayed with the increase in SI contents, and the dilution effect of SI was more prominant at lower temperatures. At 110 °C, the reaction rate was not very fast and this temperature was proper for monitoring the phase separation process. At higher temperatures, gel time was shortened due to the faster curing rate of the hybrid, and the dilution effect of SI was not obvious among different hybrids.

As shown in Scheme 1b and 1c, the silanol group of SI could undergo self-condensation, and react with phenolic hydroxyl group or Si—OCH_3 attached to m-NR as well [34]. The slow self-condensation rate of SI can be indicated by the occurrence and enhancement of featured 1136 cm^{-1} signal (corresponding to Si—O—Si group) in the FTIR spectra in Fig. 5. As shown in Scheme 1c, silanol group in SI was expected to react with Si—OCH_3 or phenolic hydroxyl groups in m-NR, which could be confirmed by the disappearance of 1087 cm^{-1} signal (corresponding to Si—OCH_3) and new vibration of the Si—O-ph at 922 cm^{-1} when the hybrid was post-cured at 180 °C. The chemical bond formed between m-NR and SI could stabilize the fine dispersion. Macroscopic phase separation occurred without KH560 suggesting that KH560 played a key role in enhancing the compatibility during curing.

Table 1
Gel time for hybrids with different SI contents at different temperatures.

	110 °C	130 °C	150 °C
m-NR	352 s	237s	145 s
95-5m-NR/SI	356 s	246 s	149 s
85-15m-NR/SI	405 s	280 s	154 s
75-25m-NR/SI	578 s	406 s	161 s
65-35m-NR/SI	622 s	450 s	165 s

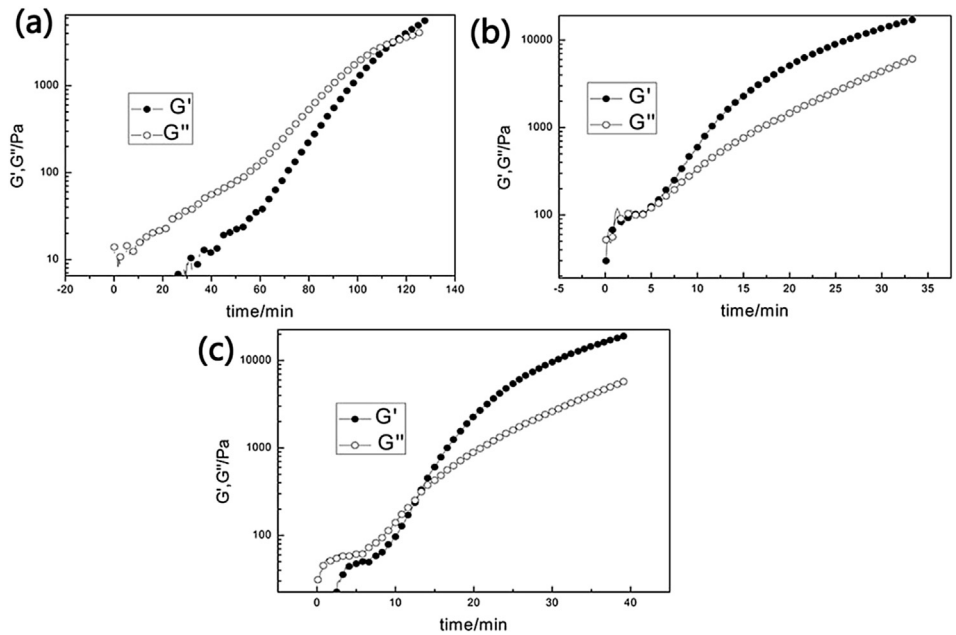

Fig. 4. Iso-thermal rheological curves of (a) SI + HMTA; (b) m-NR + HMTA; (c) 75-25m-NR/SI: storage modulus (G′) and loss modulus (G″) -time plot.

Please cite this article in press as: S. Li, et al., Enhanced compatibility and morphology evolution of the hybrids involving phenolic resin and silicone intermediate, Materials Chemistry and Physics (2015), http://dx.doi.org/10.1016/j.matchemphys.2015.07.054

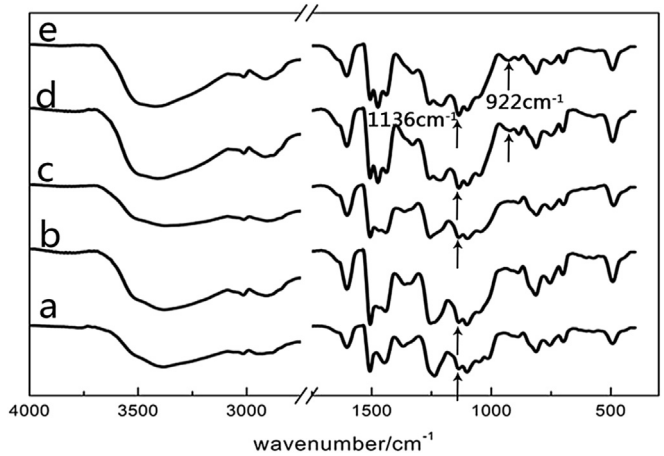

Fig. 5. FTIR spectra for 75-25m-NR/SI at different curing stages: (a) 110 °C − 10 min; (b) 110 °C − 1 h; (c) 110 °C − 5 h; (d) 110 °C − 5 h + 180 °C − 4 h; (e) 110 °C − 5 h + 180 °C − 4 h + 220 °C − 4 h.

3.3. Morphology of the hybrids

In order to investigate the morphology of the hybrids at initial curing process, the yellow transparent 75-25m-NR/SI hybrid resin was first observed by PCOM, as shown in Fig. 6a–e. Uniformly distributed micro-domains were observed throughout the sample. Optical microscopic image at 0 min was vague because of the poor contrast between the phase domains. The images became clearer and clearer with the reaction continuing, suggesting a coarsening process. The size of the domain slightly increased, and more and more bubbles generated from the curing reaction would disturb the optical microscope observation in the following processes. According to the TEM image shown in Fig. 6f, at 10 min, nanometer sized particles were dispersed in the matrix. These particles loosely aggregated and formed micron domains, which corresponded to PCOM observation. The blurred interface between the two phases indicated that the two components were successfully coupled and partially compatible at this curing stage. The fine dispersion and blurred interface could be attributed to the chemical structure illustrated in Scheme 1.

The evolution of the phase separation was investigated by performing SEM observation on the fracture surfaces. Upon curing 75-25m-NR/SI for different time at 110 °C, the samples were quenched and cracked in liquid nitrogen. Decomposition of the HMTA and curing of the phenolic resin would generate ammonia and water, while self-condensation of SI would produce methanol and water. With the curing proceeding, small holes ascribed to the gas release and sub-micron particles gradually appeared. As shown in Fig. 7a, b, the particles were found around or along the cracks, suggesting the particles were different in component with the smooth matrix. This phenomenon became more obvious when the samples were cured for 30 min, as shown in Fig. 7c. The loosely aggregated phase structure, which could be observed in PCOM and TEM, was hard to be found in SEM image due to the low contrast of the two components. At 120 min, the particles grew larger, while small holes can seldom be found over the matrix. The particles might be formed from the further aggregation and compaction of the initial loosely aggregated domains. At 180 min, the roughness of the matrix was much more developed. The nanoparticles grew larger and transformed into irregular ovals, and the interface was clearly developed. These phenomena suggested the decreased miscibility between the two phases. Besides the sub-micron particles, uniformly distributed nanoparticles (around 20–30 nm in size) could be observed in the matrix. The coexistence of particles in different scales was confirmed by TEM observation as shown in Fig. 7(h). The high acceleration voltage made the ultrathin sections deformed, resulting in the change of the particle shape. The smaller particles were similar with those observed in image taken at early curing time (10 min, Fig. 6f), but larger in size, and this indicated that the

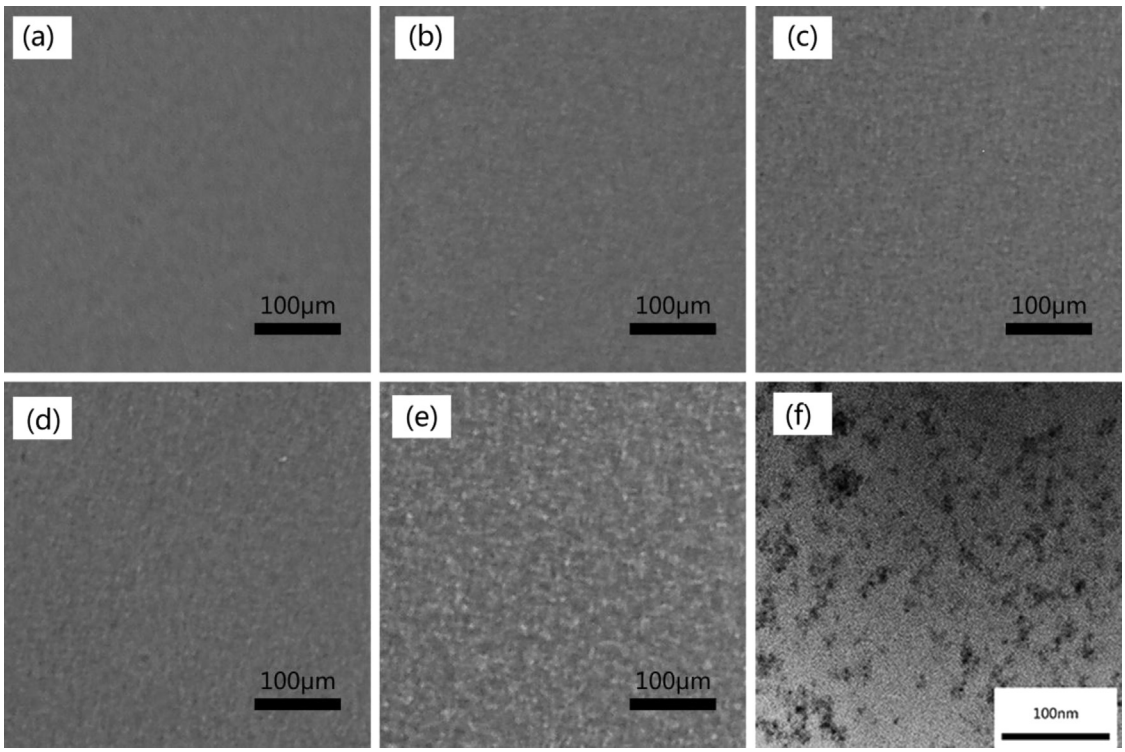

Fig. 6. Images of the 75-25m-NR/SI at preliminary curing stage (a) PCOM at 110 °C for 0 min; (b) 3 min; (c) 5 min (d) 9 min (e)14 min (f) TEM at 110 °C for 10 min.

Please cite this article in press as: S. Li, et al., Enhanced compatibility and morphology evolution of the hybrids involving phenolic resin and silicone intermediate, Materials Chemistry and Physics (2015), http://dx.doi.org/10.1016/j.matchemphys.2015.07.054

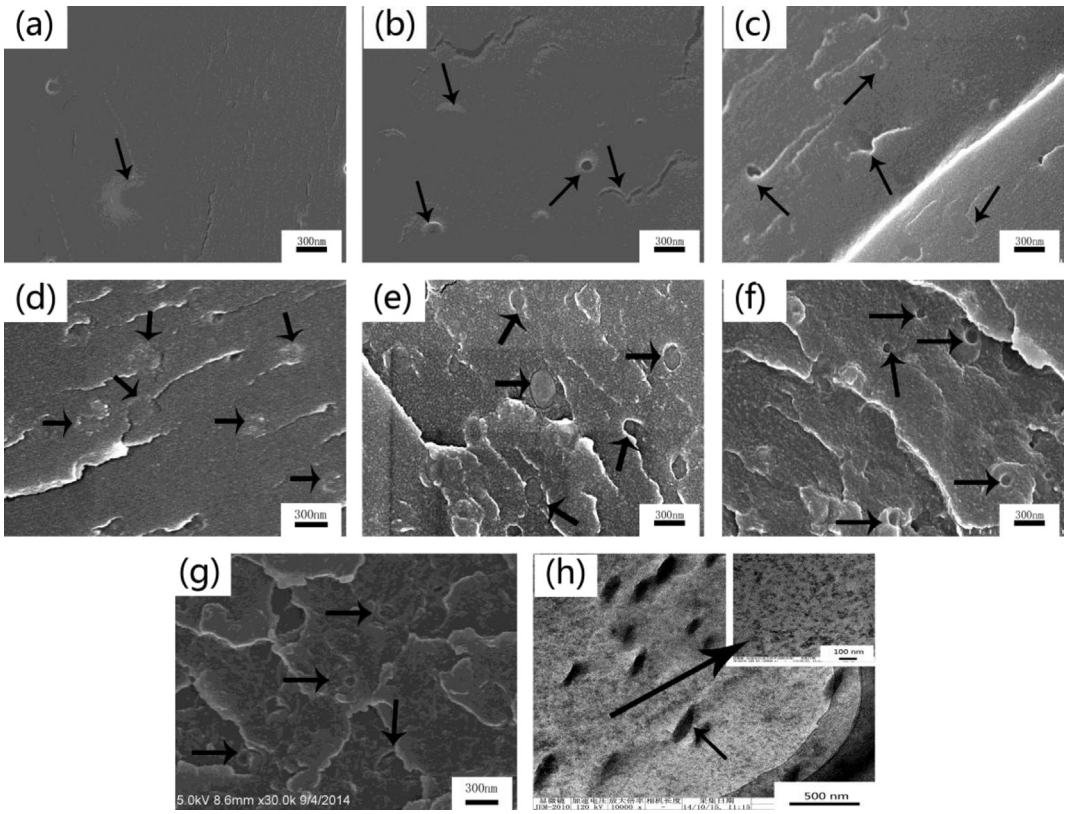

Fig. 7. SEM images of 75-25m-NR/SI after different curing time at 110 °C (a) 5 min; (b) 10 min; (c) 30 min; (d) 120 min; (e) 180 min; (f) 220 min; (g) 600 min; (h) TEM images at 180 min.

loosely aggregated domains always exist during the curing. At 220 min, roughness of the matrix was not further changed, while newly-generated holes in few tens of nanometers on the surface of the sub-micron particles can be observed in Fig. 7f. As the curing proceeding, these nano-holes gradually decreased in quantity and almost vanished at 600 min. This phenomenon will be explained later.

The phase separation mechanism was depicted as follows. Upon heating to the curing temperature, only small amount of gas was released and this period was usually called induction period, during which small holes gradually appeared in the matrix. With the curing reaction proceeding, the molecular weight of m-NR increased, and crosslink network was formed. The mixing entropy was thus decreased and the finely dispersed SI-rich nano-particles coarsened and formed loosely aggregated domains. Here, the small holes may act as the nuclei for the coarsening process due to their low interfacial energy. Since the phase separation was not a critical nucleation and growth in mechanism, the location of the particle phase domains was decided by the randomly distributed holes. The self-condensation of SI compacted the SI-rich particles and cleared the interface, and made the domains visible in SEM. However, not all of the SI-rich nano-particles got the chance to grow to micro-particles, and particles of two scales coexisted throughout the whole curing. The existence of the smaller nano-particles was speculated to be caused by the enhanced compatibility between the components as illustrated in the chemical structure characterization (Figs. 1 and 2). The sharp interface between the larger particles and the matrix indicated that as the SI particles grew to be micro-scale, their compatibility with the matrix significantly decreased. Volume shrinkage caused by the polycondensation of SI also contributed to the enhanced segregation.

At the late curing stage, HMTA almost completely decomposed, while polycondensation of SI kept releasing gas, and the released gas generated holes on the separated sub-micron particles. Given longer curing time, the gas could get out and the holes disappeared with the movement of the SI molecular chains. If cured at high temperatures, the particle-hole structure would be fixed by the enhanced reaction and high crosslinking density of SI-rich phase.

It was interesting to observe the above morphology evolution after the hybrid was gelled, which was unique from other thermoset systems. The main reason was the fairly low conversion of m-NR and the dilution effect of SI on the crosslinking network. The continuous gas release may also enhance the mobility of the phase domains and promote the phase coarsening in this system.

Stepwise curing process is usually carried out to ensure complete curing. The hybrids were cured following 80 °C-4 h +120 °C-2 h +180 °C-4 h and the fracture surface morphology after each curing stage was shown in Fig. 8. When the sample was cured at the initial stage, 80 °C, HMTA did not decompose and the reaction of m-NR was quite slow, thus compact and smooth surface was observed. As curing went on, the surface gradually became rough, suggesting the occurrence of structure coarsening. Sub-micron particles were formed after the sample was cured at 120 °C for 2 h. The quantity and size of the particles increased after sample being cured at 180 °C for 1 h, while the interface between the particles and matrix was much sharper than before. Particle-hole structure could be observed in the sample cured at 180 °C for a longer time. The structure could be fixed when cured at 180 °C due to the rapid curing rate and high crosslinking density. Curing rate significantly changed the initial phase structure and eventually affects the quantity of the sub-micron SI-rich particles.

Fracture surface of the cured hybrids with various SI contents

Please cite this article in press as: S. Li, et al., Enhanced compatibility and morphology evolution of the hybrids involving phenolic resin and silicone intermediate, Materials Chemistry and Physics (2015), http://dx.doi.org/10.1016/j.matchemphys.2015.07.054

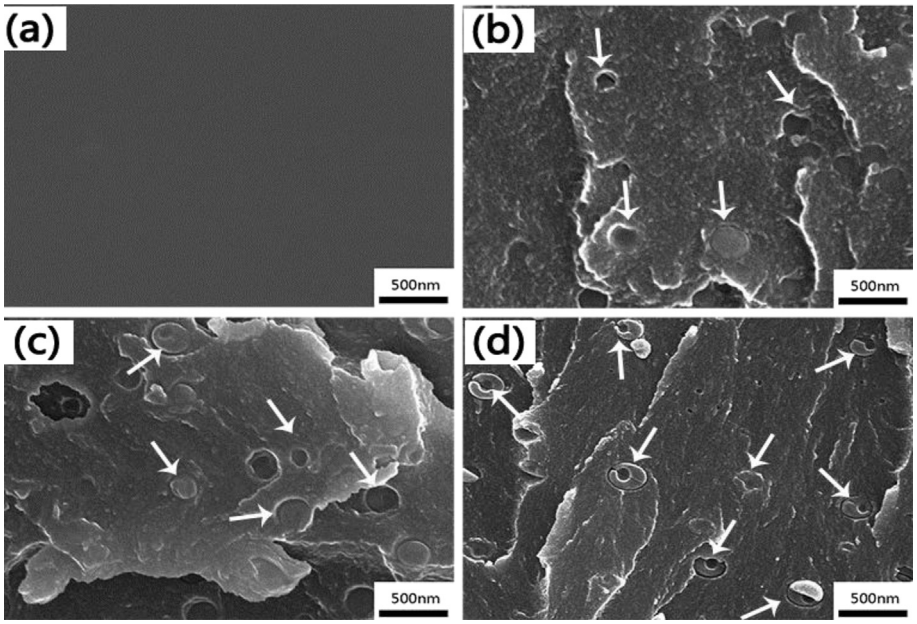

Fig. 8. SEM images of 75-25m-NR/SI after curing at (a) 80 °C-4 h (b) 80 °C-4 h +120 °C-2 h; (c) 80 °C-4 h +120 °C-2 h +180 °C-1 h; (d) 80 °C-4 h +120 °C-2 h +180 °C-4 h.

was observed by SEM, and the corresponding images were shown in Fig. 9. NR or samples with less than 5 wt% SI loading, possessed a compact surface, while the roughness of the hybrid sample increased. The compact surface indicated the very fine dispersion of the SI-rich phase in the m-NR matrix. At high SI loading, micro- and nano-particles could be observed, and the quantity of the large particles increased with the increase in SI contents. When SI loading increased to 35%, the number of large particles increased, and the average diameter of the particles was about 1 micron; while the quantity of nano-particles decreased when compared with that of samples with 15% and 25% SI loading. The higher SI concentration increased the collision of the nano-particles during curing, and promoted the aggregation and merging of these particles. To further indicate the chemical structure of the dispersed phase, 65-35m-NR/SI was etched by THF. Since SI can be swelled and removed by THF, the appearance of etched holes proved that the dispersed phase was SI-rich.

3.4. Thermal property of the cured hybrid resin

TGA measurements were conducted under nitrogen to evaluate the thermal stability of cured m-NR/SI hybrid resins, and the results were shown in Fig. 10 and Table 2. The thermal stability was improved with the increase of SI contents. The 5% mass loss temperature, $T_{5\%}$, and char yield at 900 °C of the cured 75-25m-NR/SI resin were 356.6 °C and 67.78%, respectively, which was about 76 °C and 9% higher than those of cured NR. Temperature at the maximum loss rate of the cured 75-25m-NR/SI resin was 590.0 °C, about 50 °C higher than that of cured NR resin. When the SI content reached 35%, the initial decomposition temperature is slightly decreased. The relationship between the thermal stability and the structure will be discussed later.

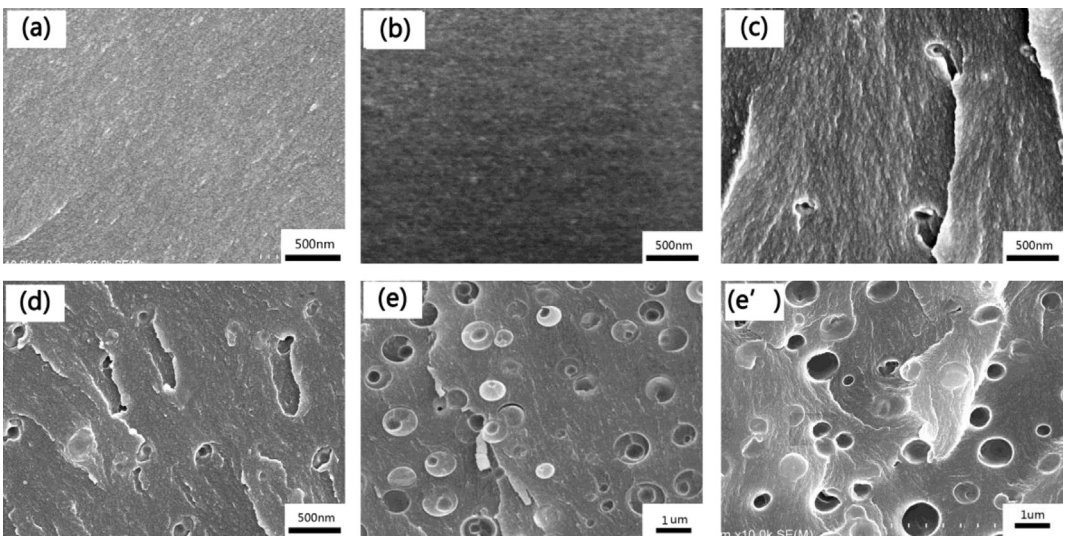

Fig. 9. SEM images of m-NR/SI hybrids with different SI weight fractions, (a) pure NR; (b) 95-5m-NR/SI; (c) 85-15m-NR/SI; (d) 75-25m-NR/SI; (e) 65-35m-NR/SI; (e') 65-35m-NR/SI after THF etched.

Please cite this article in press as: S. Li, et al., Enhanced compatibility and morphology evolution of the hybrids involving phenolic resin and silicone intermediate, Materials Chemistry and Physics (2015), http://dx.doi.org/10.1016/j.matchemphys.2015.07.054

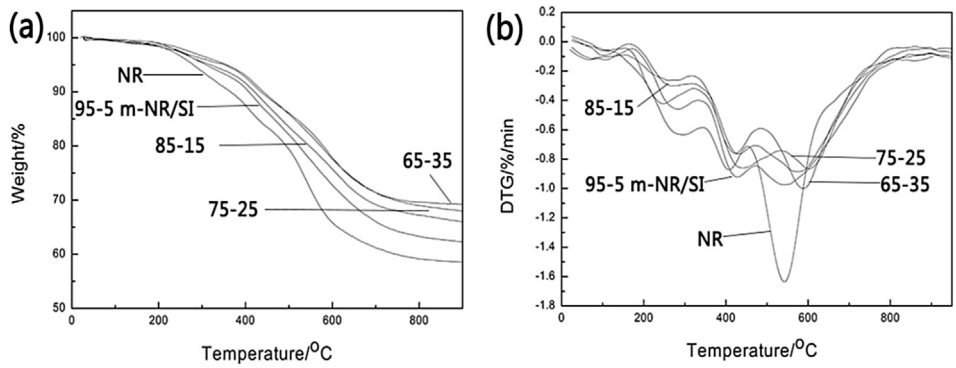

Fig. 10. TGA curves of cured NR resin and m-NR/SI hybrids in nitrogen (a) Residual weight–temperature curves; (b) Derivative thermal gravimetric curves (DTG).

Table 2
TGA results for NR and m-NR/SI hybrids.

	NR	95-5m-NR/SI	85-15m-NR/SI	75-25m-NR/SI	65-35m-NR/SI
5%weight loss temperature (°C)	279.8	309.1	318.4	356.6	351.3
10%weight loss temperature (°C)	365.4	407.5	420.7	440.8	435.4
900 °C residual Weight	58.51%	62.26%	65.97%	67.78%	69.22%
DTAmax (°C)	542.8	531.3	596.2	590.0	589.3

Oxidation resistance of the hybrids was measured with a high temperature oxidation test performed in a muffle furnace. The carbon retention was calculated by equation (1). As listed in Table 3, the carbon retention increased to 65.5% when SI loading was 15% and decreased as SI contents further increased. At 35% SI loading, the slightly decreased carbon retention suggested that separated spherical SI particles could not effectively protect the carbon element from oxidation [26].

$$C = A \cdot C_1 / C_2 * 100\% \quad (1)$$

Where C is the carbon retention (%) after thermal oxidation, A is the mass retention (%), C_1 and C_2 correspond to the carbon content (%) after oxidation and after curing.

SI was expected to improve the thermal stability of the phenolic resin, due to its intrinsic excellent oxidation resistance. It can be inferred that when the SI loading is 15% or less, most SI can be molecularly or in nanometer size dispersed in the phenolic matrix and the interfacial was relatively blurred. The SI was hard to be oxidized, providing an insulating layer to reduce the oxygen diffusion into the phenolic matrix [2,26,29]. Hence, the carbon matrix was protected from oxidation and carbon retention was increased. With more than 25% SI loading, segregation between SI and m-NR became more severe, and more SI would be separated from the matrix. Larger SI-rich particles with much sharper interface were formed and existed as separated particles. Moreover, the existing gap between the two phases suggested the weak interaction between the two components. The gap generated at high SI loading would act as defects for oxygen diffusion, and prohibited the protection of phenolic resin from oxidation. The fine dispersion with enhanced compatibility provided better effectiveness in improving the thermal oxidation, when compared with the separated domains [26]. The application of the hybrids in high temperature field was enhanced due to the improved thermal stability and oxidation resistance. This material is potentially applicable as binders for refractories and as resin matrix for anti-ablative composites.

4. Conclusions

The hybrid resin m-NR/SI has been developed based on novolac resin and silicone intermediate. Compatibility was enhanced and morphology evolution during the curing of hybrid resins was investigated and discussed in detail. Tiny aggregates composed of few tens of nanometer particles were formed and finely dispersed in the initial mixture and further coarsened during curing. Not all of the nano-particles grew into micro-particles, and particles of two scales coexisted in the cured sample. Unique particle-hole structure was formed during the phase coarsening, which can be relaxed with the proceeding aggregation or fixed by the rapid curing rate. Thermal stability of novolac phenolic resin was significantly improved, and oxidation resistance was also slightly enhanced. The fine dispersion with enhanced compatibility provided better effectiveness in improving the thermal oxidation, when compared with the separated domains.

Table 3
Carbon retention after thermal oxidation at 650 °C for 30 min in muffle.

Sample name	Mass retention (%)	Carbon content before oxidation (%)	Carbon content after oxidation (%)	Carbon retention (%)
NR	52.85	76.71	91.04	62.72
95-5m-NR/SI	54.70	74.25	87.46	64.43
85-15m-NR/SI	58.00	72.58	81.99	65.52
75-25m-NR/SI	58.05	72.28	76.38	61.34
65-35m-NR/SI	58.65	71.36	72.17	59.32

Please cite this article in press as: S. Li, et al., Enhanced compatibility and morphology evolution of the hybrids involving phenolic resin and silicone intermediate, Materials Chemistry and Physics (2015), http://dx.doi.org/10.1016/j.matchemphys.2015.07.054

Acknowledgement

The authors gratefully acknowledge the financial support of the National Natural Science Foundation of China (No. 51473171 & No. 51403218).

References

[1] H. Li, D. Yao, Q. Fu, L. Liu, Y. Zhang, X. Yao, Y. Wang, H. Li, Carbon 52 (2013) 418.
[2] Y. Badhe, K. Balasubramanian, RSC Adv. 4 (2014) 28956.
[3] S.G. Kang, J.H. Hong, C.K. Kim, Ind. Eng. Chem. Res. 49 (2010) 11954.
[4] T. Takeichi, T. Kawauchi, T. Agag, Polym. J. 40 (2008) 1121.
[5] Y. Chen, C. Hong, P. Chen, RSC Adv. 3 (2013) 13734.
[6] M.O. Abdalla, A. Ludwick, T. Mitchell, Polymer 44 (2003) 7353.
[7] J. Gao, L. Xia, Y. Liu, Polym. Degrad. Stab. 83 (2004) 71.
[8] M. Spontón, J.C. Ronda, M. Galià, V. Cádiz, Polym. Degrad. Stab. 94 (2009) 145.
[9] K. Haraguchi, Y. Usami, K. Yamamura, S. Matsumoto, Polymer 39 (1998) 6243.
[10] Y. Zhang, S. Lee, M. Yoonessi, K. Liang, C.U. Pittman, Polymer 47 (2006) 2984.
[11] C.-L. Chiang, C.-C.M. Ma, Polym. Degrad. Stab. 83 (2004) 207.
[12] J.C. Cabanelas, B. Serrano, M.G. Gonzalez, J. Baselga, Polymer 46 (2005) 6633.
[13] B. Montero, R. Bellas, C. Ramírez, M. Rico, R. Bouza, Compos. Part B 63 (2014) 67.
[14] Y. Liu, K. Zeng, S. Zheng, React. Funct. Polym. 67 (2007) 627.
[15] Y. Zhang, C. Shang, X. Yang, X. Zhao, W. Huang, J. Mater. Sci. 47 (2012) 4415.
[16] N. Furukawa, M. Yuasa, Y. Kimura, Polymer 40 (1999) 1853.
[17] N. Furukawa, M. Yuasa, Y. Yamada, Y. Kimura, Polymer 39 (1998) 2941.
[18] L. Mascia, A. Kioul, Polymer 36 (1995) 3649.
[19] E. Yilgör, İ. Yilgör, S. Süzer, Polymer 44 (2003) 7271.
[20] J. Choi, S.G. Kim, R.M. Laine, Macromolecules 37 (2004) 99.
[21] J. Choi, A.F. Yee, R.M. Laine, Macromolecules 36 (2003) 5666.
[22] L. Matějka, A. Strachota, J. Pleštil, P. Whelan, M. Steinhart, M. Šlouf, Macromolecules 37 (2004) 9449.
[23] C.-L. Chiang, C.-C.M. Ma, D.-L. Wu, H.-C. Kuan, J. Polym. Sci. Part A Polym. Chem. 41 (2003) 905.
[24] T.-H. Ho, C.-S. Wang, Eur. Polym. J. 37 (2001) 267.
[25] Y. Ni, S. Zheng, K. Nie, Polymer 45 (2004) 5557.
[26] Y.-J. Lee, J.-M. Huang, S.-W. Kuo, J.-K. Chen, F.-C. Chang, Polymer 46 (2005) 2320.
[27] L. Wang, S. Zheng, Polymer 51 (2010) 1124.
[28] G. Hernandezpadron, F. Rojas, M. Garciagarduno, M. Canseco, V. Castano, Mater. Sci. Eng. A 355 (2003) 338.
[29] M.R. Schütz, K. Sattler, S. Deeken, O. Klein, V. Adasch, C.H. Liebscher, U. Glatzel, J. Senker, J. Breu, J. Appl. Polym. Sci. 117 (2010) 2272.
[30] X. Sun, Y. Xu, D. Jiang, D. Yang, D. Wu, Y. Sun, Y. Yang, H. Yuan, F. Deng, Colloids Surf. Physicochem. Eng. Asp. 289 (2006) 149.
[31] J.M. Lin, C.C.M. Ma, F.Y. Wang, H.D. Wu, S.C. Kuang, J. Polym. Sci. Part B Polym. Phys. 38 (2000) 1699.
[32] R.H. Horst, H.H. Winter, Macromolecules 33 (2000) 130.
[33] J. Wan, S. Wang, C. Li, D. Zhou, J. Chen, Z. Liu, L. Yu, H. Fan, B.-G. Li, Thermochim. Acta 530 (2012) 32.
[34] Kane, United States Pat., 5736619 (1998).

Please cite this article in press as: S. Li, et al., Enhanced compatibility and morphology evolution of the hybrids involving phenolic resin and silicone intermediate, Materials Chemistry and Physics (2015), http://dx.doi.org/10.1016/j.matchemphys.2015.07.054